



## Original Article

# Human umbilical cord mesenchymal stem cells protect MC3T3-E1 osteoblasts from dexamethasone-induced apoptosis via induction of the Nrf2-ARE signaling pathway

Chen Qiu<sup>a</sup>, Zhaowen Li<sup>a,1</sup>, Puji Peng<sup>b,\*</sup><sup>a</sup> Department of Sports Medicine, The Affiliated Hospital of Wuhan Sports University, Wuhan, 430000, China<sup>b</sup> Department of Orthopedics, Henan Provincial People's Hospital, Zhengzhou, 450003, China

## ARTICLE INFO

## Article history:

Received 11 November 2023

Received in revised form

29 January 2024

Accepted 25 February 2024

## Keywords:

Human umbilical cord mesenchymal stem cell

Dexamethasone

Nrf2-ARE signaling pathway

Apoptosis

Oxidative stress

## ABSTRACT

**Objective:** To investigate the protective effect human umbilical cord mesenchymal stem cells (hUC-MSCs) have on Dexamethasone (Dex)-induced apoptosis in osteogenesis via the Nrf2-ARE signaling pathway.

**Methods:** Glucocorticoid-induced osteonecrosis of the femoral head (GC-ONFH) was developed in rats through the administration of lipopolysaccharide and methylprednisolone. The incidence of femoral head necrosis, cavity notch, apoptosis of osteoblasts, and bone density were observed by HE staining, TUNEL staining, and Micro-CT. hUC-MSCs were co-cultured with mouse pre-osteoblast MC3T3-E1. The survival rate of osteoblasts was determined by CCK8, and apoptosis and ROS levels of osteoblasts were determined by flow cytometer. The viability of antioxidant enzymes SOD, GSH-Px, and CAT was analyzed by biochemistry. Nrf2 expression levels and those of its downstream proteins and apoptosis-related proteins were analyzed by Western blotting.

**Results:** In rats, hUC-MSCs can reduce the rates of empty bone lacuna and osteoblast apoptosis that are induced by glucocorticoids (GCs), while reducing the incidence of GC-ONFH. hUC-MSCs can significantly improve the survival rate and antioxidant SOD, GSH-Px, and CAT activity of MC3T3-E1 cells caused by Dex, and inhibit apoptosis and oxidative stress levels. In addition, hUC-MSCs can up-regulate the expression of osteoblast antioxidant protein Nrf2 and its downstream protein HO-1, NQO-1, GCLC, GCLM, and apoptosis-related protein bcl-2, while also down-regulating the expression of apoptosis-related protein bax, cleaved caspase-3, cleaved caspase-9, and cytochrome C in MC3T3-E1 cells. hUC-MSCs improve the ability of MC3T3-E1 cells to mineralize to osteogenesis. However, the promoting effects of hUC-MSCs were abolished following the blocking of the Nrf2-ARE signaling pathway for osteoblasts.

**Conclusion:** The results reveal that hUC-MSCs can reduce Dex-induced apoptosis in osteoblasts via the Nrf2-ARE signaling pathway.

© 2024, The Japanese Society for Regenerative Medicine. Production and hosting by Elsevier B.V. This is an open access article under the CC BY-NC-ND license (<http://creativecommons.org/licenses/by-nc-nd/4.0/>).

## 1. Introduction

Necrosis of the femoral head that is caused by long-term high-dose glucocorticoid use is known as glucocorticoid-induced osteonecrosis of the femoral head (GC-ONFH). Clinical observation has found that the majority of GC-ONFH patients have severe hip pain and develop lameness within a few years. A large area of osteogenic

necrosis can then appear, and cavity and joint collapse can occur in the femoral head. Total hip replacement is eventually required [17,20].

Mesenchymal stem cells (MSCs) are a class of multifunctional cells that differentiate into a variety of cells. MSCs can produce cytokines for the regulation of immunity and the promotion of tissue repair and anti-apoptosis [15,22,27,29]. These properties

\* Corresponding author.

E-mail addresses: [pengpuji@126.com](mailto:pengpuji@126.com), [3816072961@qq.com](mailto:3816072961@qq.com) (P. Peng).

Peer review under responsibility of the Japanese Society for Regenerative Medicine.

<sup>1</sup> These authors contributed equally to this work.

make MSCs stand out in studies on femoral head necrosis treatment. The aim of this study is to investigate the protective effect and mechanism of human umbilical cord mesenchymal stem cells (hUC-MSCs) on Dexamethasone (Dex)-induced osteoblasts apoptosis via the Nrf2-ARE signaling pathway.

## 2. Materials and methods

### 2.1. GC-ONFH animal model and groupings

The animal study protocol was approved by the Wuhan University Ethics Committee (number: 20180920). 30 male Sprague-Dawley rats with approximate weights of  $360 \pm 26$  g, that were 28 weeks old were purchased from Beijing Vital River Laboratory Animal Technology Co. Ltd. The rats were randomly divided into three groups of control group, model group, and treatment group. The rats in the control group received only 0.9% of the tail vein saline injection within one week. The rats in the model group were administered with 2 mg/kg of lipopolysaccharide (Sigma-Aldrich, USA) intravenously once daily for two days and injected with 20 mg/kg of methylprednisolone (Pfizer, USA) intramuscularly once daily for five days. The procedure for the treatment group was similar to that of the model group, apart from the fact that  $1 \times 10^6$  hUC-MSCs (Shenzhen Wingor Bio-technology Co., Ltd., China) were injected into the tail vein 1 h following the intramuscular injection of methylprednisolone. The femoral head samples and venous blood of the rats were removed under anesthesia after 28 days of rearing and then used for further analysis.

### 2.2. Hematoxylin and eosin (HE) staining

The femoral heads were fixed in 10% paraformaldehyde (pH = 7.4) for 24 h and then in 10% ethylenediamine tetraacetic acid (pH = 7.4) for 2 months to ensure decalcification. The decalcified samples were then dehydrated in gradient alcohol before being embedded in paraffin. The paraffins were sliced into 4  $\mu$ m sections, dewaxed in xylene, and hydrated in gradient alcohol. Sections were stained with hematoxylin for 6 min and eosin for 2 min. The necrosis of the femoral head was diagnosed as bone trabecular fracture or decrease, empty bone socket, and nuclear consolidation increase.

### 2.3. TdT-mediated dUTP Nick-End Labeling (TUNEL) staining

The paraffins in the last step were sliced into 4  $\mu$ m sections, dewaxed in xylene, and hydrated in gradient alcohol. Section staining was performed in accordance with the instructions of the In Situ Cell Death Detection Kit (Roche, Basel, Switzerland). The osteoblast nuclei with brown staining were considered apoptotic cells under a microscope.

### 2.4. Detection of alkaline phosphatase (ALP) activity

In order to detect ALP activity in the serum, blood samples of 1–2 mL were drawn from the tail veins of rats and centrifuged for 10 min at 1500 r/min at 4 °C. The separated serums were used for testing ALP activity. For ALP activity in osteoblasts, osteoblasts were harvested and seeded into a 24-well plate and then treated with 100  $\mu$ L of lysis buffer after washing. An ALP assay kit (Nanjing Jiancheng, A059-2) was used for measuring ALP activity.

### 2.5. Detect the distribution of hUC-MSCs in rats

$1 \times 10^5$  hUC-MSCs were seeded on 24-well culture plates. When the cells reached about 70%, CMV-Luc2-T2A-Puro Lentivirus

(Oligobio, OGL-LVXH-001) were transfected for 48 h then selected by puromycin (Solarbio, P8230). Stable transplanted cells were obtained after 2 weeks.

Transfected hUC-MSCs were injected into both groups of rats from day three to day seven days through the tail vein. There were 6 rats divided into two groups. The control group will not have any treatment. The modeling of the model group is the same as that method in 2.1. The whole body luminescence signal was observed on the first day, the third day and the seventh day after modeling by using Luznoche® B animal live imaging system (SpectralMagic).

### 2.6. Cell culture

Bone tissues from healthy adult rats were collected after anesthesia. They were cut into fragments, digested with trypsin for 5 min, and neutralized with serum-containing medium. The cells were centrifuged and then incubated with 0.1% collagenase for 30 min. Primary osteoblasts were collected and cultured at 37 °C and 5% CO<sub>2</sub> with Ham's F-12 medium containing 10% FBS. All of the procedures were performed using second to fifth-generation osteoblasts. The osteoblasts were divided into control and Dex groups.

The stem cells used in the experiment were P4 generation hUC-MSCs that were provided by Shenzhen Yinguan Biotechnology Co. China. Mouse pre-osteoblast cells MC3T3-E1 were purchased from the Cell Bank of the Chinese Academy of Sciences, Shanghai.

In order to investigate the effect hUC-MSC has on MC3T3-E1 cells induced by Dex, MC3T3-E1 cells were divided into five groups: control group (MC3T3-E1), model group (MC3T3-E1 + Dex), inhibitor group (MC3T3-E1 + Dex + ML385), co-culture group (hUC-MSCs + MC3T3-E1 + Dex), and co-culture + inhibitor group (hUC-MSCs + MC3T3-E1 + Dex + ML385).

The MC3T3-E1 cells were maintained in DMEM medium (HyClone, SH30022) supplemented with 10% fetal bovine serum (FBS) and 1% antibiotics (streptomycin/penicillin). MC3T3-E1 cells in the log growth phase that were digested with trypsin were seeded in the lower chamber of a Transwell plate. Following 24 h of incubation, the medium that contained 1  $\mu$ M of Dex (sigma, D4902) was replaced except for the control group. 5  $\mu$ M concentration of ML385 (Selleck, S8790) was added to the inhibitor group and co-culture + inhibitor group. The hUC-MSCs were inoculated in the upper chamber of the Transwell plate with DMEM/F12 medium (HyClone, SH30023) supplemented with 10% FBS and antibiotics in the co-culture group and co-culture + inhibitor group.

### 2.7. Cell viability assay

The viabilities of osteoblasts or MC3T3-E1 cells in each group were detected using cell counting kit-8 (CCK-8) assay (Beyotime, C0038). CCK8 solution was added to each well for 10  $\mu$ L and then incubated for 2 h. The absorption values at 450 nm in each well were measured using a microplate reader (Diatek, DR-200Bs) and survival rate was calculated.

### 2.8. Cell proliferation

Osteoblasts were harvested and seeded into a 24-well plate. 5-bromo-2'-deoxyuridine (BrdU) solution was added dropwise to each well for 3 h before Dex application to determine cell proliferation.

### 2.9. Western blotting

Osteoblasts or MC3T3-E1 cells were washed three times using PBS before being lysed with the cellular total protein extraction

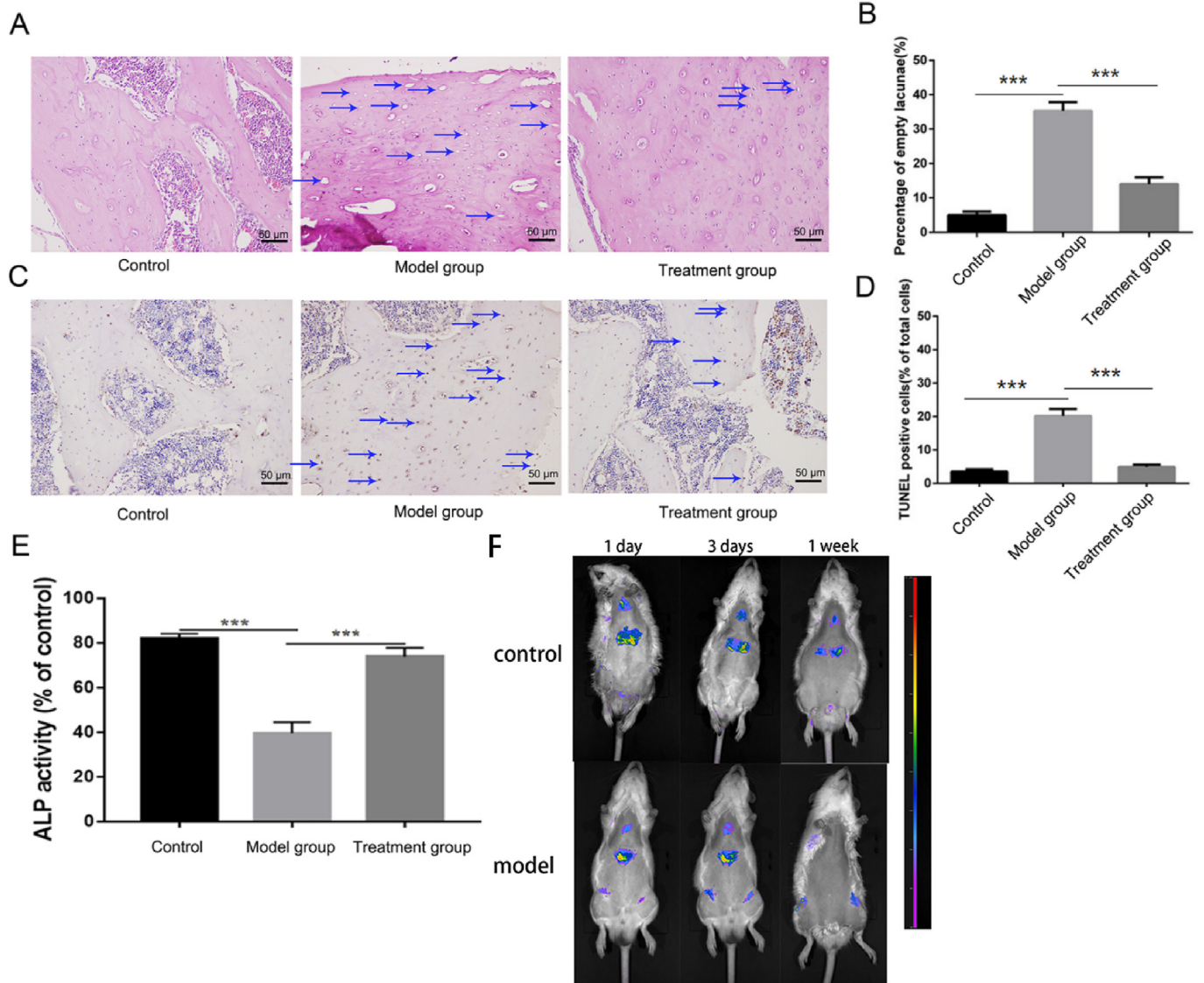


**Fig. 1.** HUC-MSCs reduced osteoblast apoptosis and promoted osteogenesis on GC-ONFH. (A) HE staining of rat femoral heads receiving different treatments – blue arrows indicate empty lacunae (Scale bar = 50  $\mu$ m). (B) Quantitative analysis of empty lacuna rate in (A),  $n = 3$ . (C) TUNEL staining of the rat femoral head tissue – blue arrows indicate apoptotic cells (Scale bar = 50  $\mu$ m). (D) Quantitative analysis of the rate of TUNEL-positive cells in (C),  $n = 3$ . (E) ALP activity in the three groups,  $n = 3$ . (F) Distribution of hUC-MSCs in rats of control and model group,  $n = 3$ .

reagent for 5 min and centrifuged at 4  $^{\circ}$ C, 12,000 g for 10 min. The supernatant that was total protein solution was removed. Sample protein concentrations were determined using the BCA Protein Concentration Assay kit (ASPEN, AS1086), and separation glue and concentrated gel were prepared for the sodium dodecyl sulfate polyacrylamide gel electrophoresis (SDS-PAGE). An equal amount of protein samples was loaded onto SDS-PAGE gel and then subjected to electrophoresis. The proteins on gels were transferred to polyvinylidene difluoride (PVDF) membranes that were then blocked in nonfat milk for 1 h. The membranes were incubated overnight with different monoclonal primary antibodies: anti-Bax (rabbit, 1:2000, CST, #2772), anti-Bcl-2 (rabbit, 1:1000, abcam, ab196495), anti-Cleaved Caspase3 (rabbit, 1:500, affbio, AF7022), anti-Cleaved Caspase9 (rabbit, 1:500, affbio, AF5240), anti-cytochrome C (rabbit, 1:500, CST, #4280), anti-GAPDH (rabbit, 1:10000, abcam, ab181602), anti-Nrf2 (rabbit, 1:500, abcam, ab76026), anti-HO-1 (rabbit, 1:3000, proteintech, 27282-1-AP), anti-NQO1 (rabbit, 1:1000, proteintech, 11451-1-AP), anti-GCLC (rabbit 1:1000, proteintech, 12601-1-AP),

and anti-GCLM (rabbit, 1:3000, proteintech, 14241-1-AP). They were then incubated for 30 min with second antibodies (goat anti rabbit, 1:10000, ASPEN, AS1107). The membranes were placed in the dark for exposure and the bands on membranes were displayed with the imaging solution. The optical density value of bands was analyzed using AlphaEaseFC software.

### 2.10. Measurement of cell apoptosis

The apoptotic rate of MC3T3-E1 cells was detected using flow cytology. Following complete digestion by trypsin, the MC3T3-E1 cells were harvested and then centrifuged at 300 g for 5 min. The supernatant was discarded and MC3T3-E1 cells were washed three times with PBS. Following the Annexin V-FITC cell apoptosis assay kit (Sungene, AO2001-02P-H) instructions, cells were resuspended with 300  $\mu$ L of Binding Buffer and incubated against light for 10 min with 5  $\mu$ L Annexin V-FITC. After incubating against light for 5 min with 5  $\mu$ L PI, the cells were detected using a flow cytometer (BD, FACSCalibur).

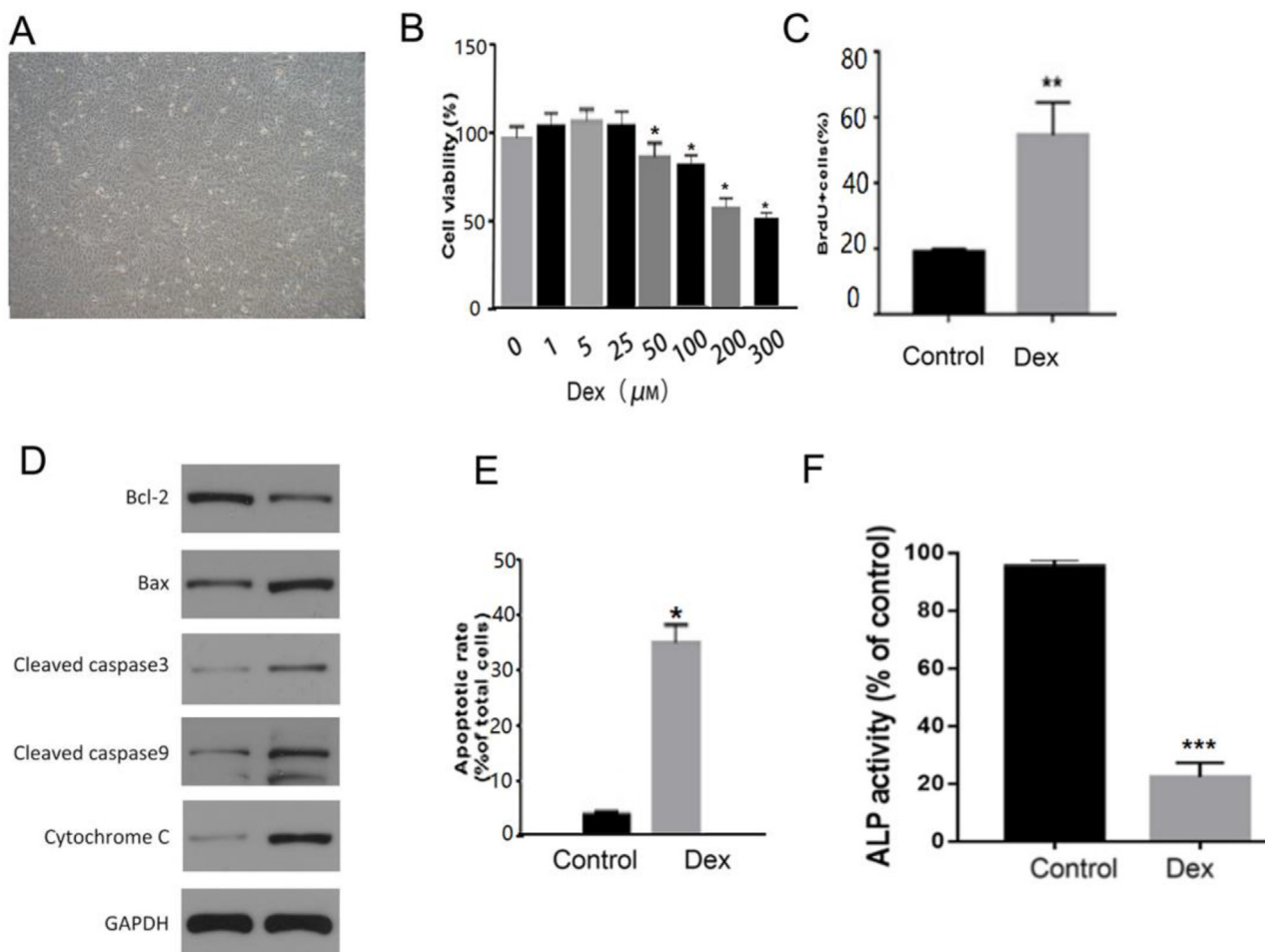


**Fig. 2.** Dex induced apoptosis of osteoblasts and inhibited osteogenesis. (A) Microscopic images of osteoblasts. (B) Viability of osteoblasts following Dex treatment (0, 1, 5, 25, 50, 100, 200, and 300 μM) for 24 h, n = 3. (C) BrdU incorporation assay, n = 3. (D) Expression levels of apoptosis-related proteins in osteoblasts. (E) TUNEL staining of osteoblasts following Dex treatment, n = 3. (F) Quantitative analysis of ALP activity, n = 3.

### 2.11. Detection of intracellular ROS level

In accordance with the instructions of the Reactive oxygen species detection kit (Beyotime, S0033), reactive oxygen species fluorescent probes (DCFH-DA) were prepared. The MC3T3-E1 cells were washed three times in PBS and incubated for 20 min with 1 mL DCFH-DA. The fluorescence intensity that indicated the level of the intracellular ROS was analyzed using a flow cytometer.

### 2.12. Viability of three enzymes: SOD, GSH-px, and CAT

The activity of antioxidant SOD, GSH-px, and CAT was evaluated by biochemical assays. MC3T3-E1 cells were washed three times with PBS and then lysed with 150 μL RIPA lysate on ice for 1 h, before being centrifuged at 4 °C, 12,000 g for 10 min. In accordance with the instructions of the three enzymes SOD, GSH-px, and CAT assay kit (Nanjing Jiancheng, A001–3, A005, A007-1), the supernatant was removed for detection.

### 2.13. Alizarin red staining

The MC3T3-E1 cells were divided into three groups: control group (MC3T3-E1), Dex group (MC3T3-E1 + Dex), and hUC-MSCs + Dex group (MC3T3-E1+ hUC-MSCs + Dex). Following

complete digestion by trypsin, MC3T3-E1 cells were harvested and centrifuged at 1300 rpm for 4 min. MC3T3-E1 Cells were fixed with paraformaldehyde for 45 min and then stained with 1 mL alizarin red for 3 min. The MC3T3-E1 Cells were observed under a microscope following alizarin red staining and then washed clean.

### 2.14. Nrf2 siRNA interference

The Nrf2 siRNA was diluted to 1 μM with 125 μL Opti-MEM (Gibco, 31985) and 5 μL Lipofectamine 2000 (ThermoFisher, 11668019) were mixed and diluted with 125 μL Opti-MEM for 5 min at room temperature. Diluted Nrf2 siRNA and diluted Lipofectamine 2000 were mixed and incubated for about 20 min at room temperature, then added to MC3T3-E1 cells that were fused to 60–70% for transfection.

### 2.15. Statistical analysis

All data was expressed as mean ± standard deviation (Mean ± SD) and analyzed using GraphPad Prism 8.0 software. Total differences were compared by ANOVA and between groups by Tukey-Kramer test. P < 0.05 was considered to be a significant difference, and \*P < 0.05, \*\*P < 0.01, \*\*\*P < 0.001, or \*\*\*\*P < 0.0001.

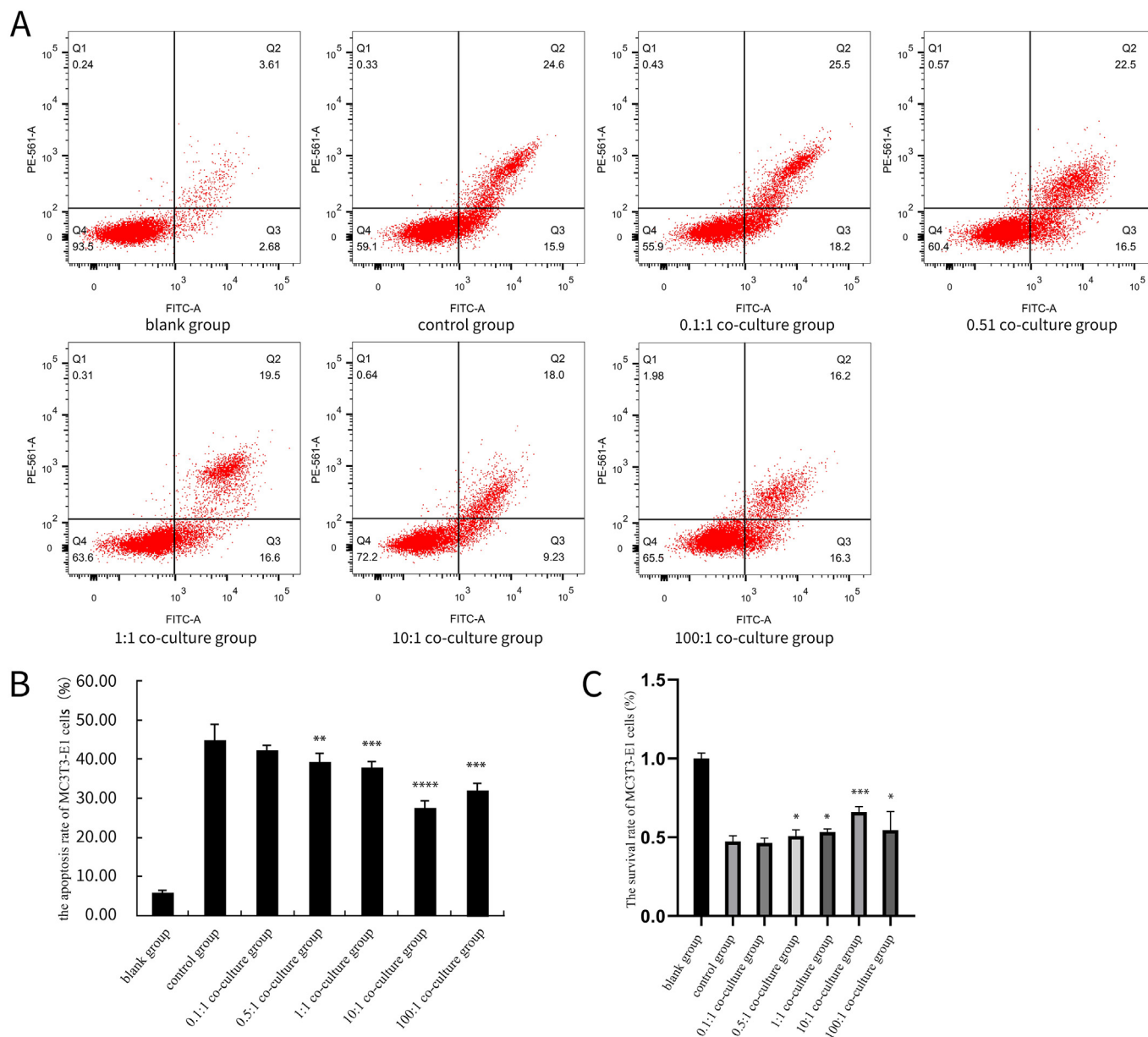


**Fig. 3.** HUC-MSCs reduced the apoptotic rate and improved the survival rate of MC3T3-E1 cells. (A) MC3T3-E1 cell apoptosis was detected by flow cytometry co-cultured with different concentrations of hUC-MSCs. (B) Quantitative analysis of apoptotic rate in (A), n = 3. (C) Survival rate of MC3T3-E1 cells co-cultured with different concentrations of hUC-MSCs, n = 3.

### 3. Results

#### 3.1. HUC-MSCs reduced the incidence of GC-ONFH and osteoblast apoptosis induced by GCs

HE staining found the incidences of necrosis of the femoral head in the control, model, and treatment groups to be 0% (0/10), 80% (8/10), and 30% (3/10), which suggests that hUC-MSCs can reduce the occurrence of GC-ONFH in rats. HE staining also demonstrated that there was no empty bone lacuna in the control group and the trabeculae arrangement was regular and intact. In comparison to the control group, the empty bone lacuna appeared widely in the model group, and the trabecular bone structure was disturbed with fracture and increased gap. In comparison to the model group, the empty bone lacuna was

significantly reduced in the treatment group, with no significant stenosis or fracture of trabecular bone (Fig. 1A). The rates of the empty bone lacuna in the control, model, and treatment groups were 5.2%, 35.6%, and 14.1% with significant difference (Fig. 1B). The results suggest that hUC-MSCs can reduce the rates of empty bone lacuna in rats.

Apoptosis of osteoblasts from the femoral heads of rats following hUC-MSCs intervention was assessed by TUNEL staining. The cells that stained brown were apoptotic cells (Fig. 1C). The rates of apoptosis in osteoblasts were 3.6%, 20.7%, and 5.1% in the control, model, and treatment groups (Fig. 1D). The rate of osteocyte apoptosis in the treatment group was found to be significantly lower than in the model group, which suggests that hUC-MSCs can reduce osteoblast apoptosis that is induced by glucocorticoids (GCs). In addition, ALP activity in the treatment group was more

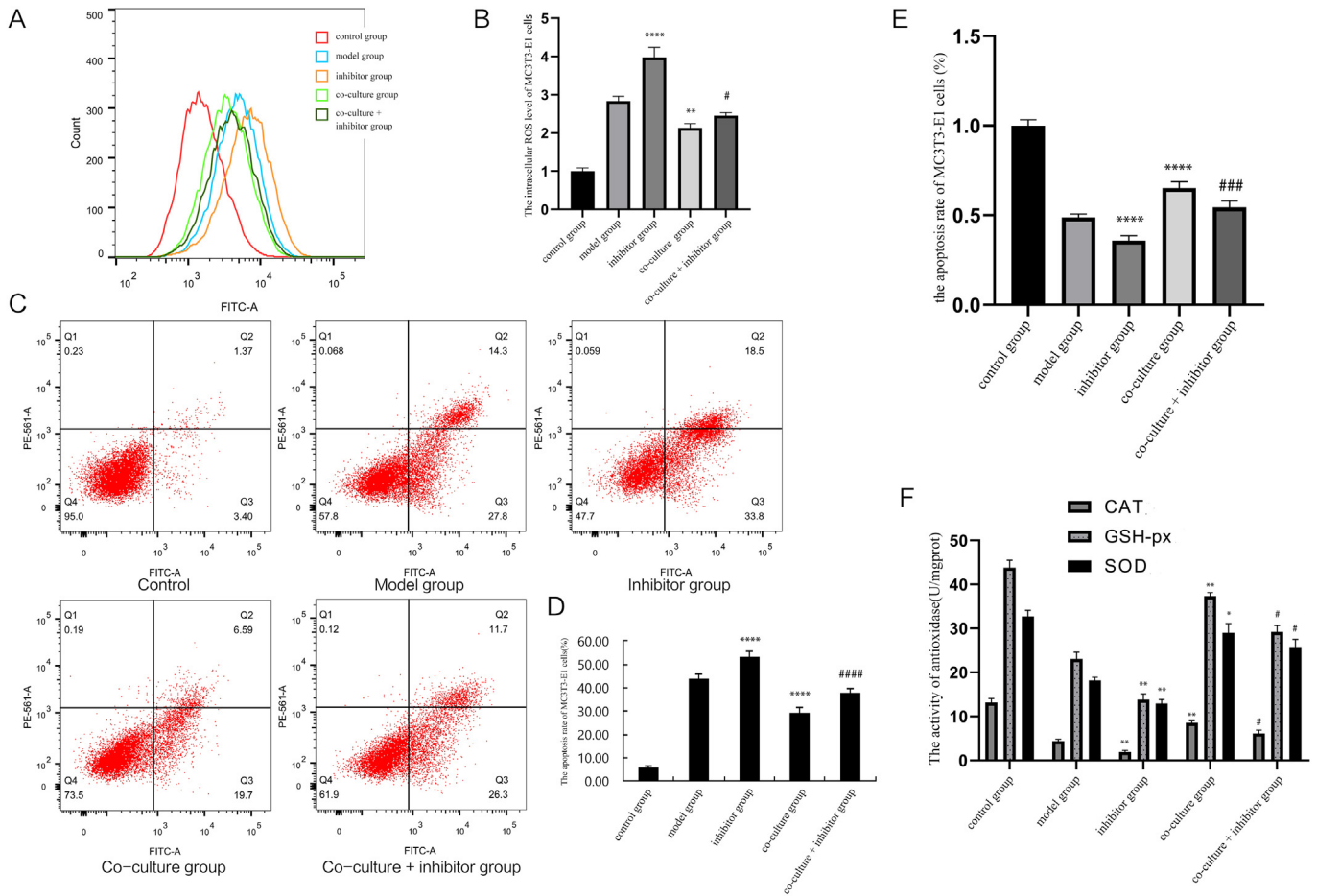


**Fig. 4.** HUC-MSCs reduced the apoptotic rate and improved the oxidative stress of MC3T3-E1 cells. (A) ROS level of MC3T3-E1 cells measured by flow cytometry. (B) Quantitative analysis of ROS levels in (A),  $n = 3$ . (C) MC3T3-E1 cell apoptosis was detected using flow cytometry. (D) Quantitative analysis of apoptotic rate in (C),  $n = 3$ . (E) Viability of MC3T3-E1 cells receiving different treatments was detected using CCK-8 assay,  $n = 3$ . (F) Activity of the oxidative stress kinases in each group,  $n = 3$ .

active than it was in the model group, but less than in the control group (Fig. 1E), which suggests hUC-MSCs improve ALP activity in serum.

Strong luminescence signals were detected in the thoracic and abdominal cavity on the first day in two group, and weak luminescence signals in the bilateral hips in the model group. On the third day, the intrathoracic and intraabdominal signals were weakened in the control and model groups, and the bilateral hip luminescence signal was slightly enhanced in the model group compared with the first day. On day 7, weak luminescence signals were detected in the intrathoracic and abdominal cavity in the control and model groups, and the bilateral hip luminescence signal was diminished in the model group compared with the third day (Fig. 1F).

### 3.2. Dex reduced viability and increased the apoptotic rate of osteoblasts

Rat primary osteoblasts were in a good growth state and were fibroblast-like (Fig. 2A). Different concentrations of Dex (0, 1, 5, 25, 50, 100, 200, and 300  $\mu\text{M}$ ) were applied to osteoblasts for 24 h as a means of investigating the effects GC has on the toxicity and viability of rat osteoblasts. CCK8 assay found Dex to reduce osteoblast viability in a dose-dependent manner. Cell viability was significantly suppressed at Dex concentrations of 100 and 200  $\mu\text{M}$ . As the osteoblasts exhibited a low survival rate with a concentration of 200  $\mu\text{M}$  (Fig. 2B), the concentration of 100  $\mu\text{M}$  was chosen

for subsequent experiments. With BrdU proliferation experiments, TUNEL staining, and ALP assay, it was found that Dex significantly inhibited the proliferation ability of osteoblasts (Fig. 2C), increased the apoptotic rate of osteoblasts (Fig. 2E), and reduced ALP activity (Fig. 2F). In addition, Western blotting showed that the expression levels of apoptosis-related proteins Bax, cleaved-caspase-3, cleaved-caspase-9, and cytochrome C in the Dex group were significantly up-regulated, while the Bcl-2 expression levels were down-regulated (Fig. 2D).

### 3.3. Determination of the optimal co-culture concentration of hUC-MSCs

After the MC3T3-E1 cells had been treated with Dex for 24 h, different concentrations of hUC-MSCs were co-cultured with MC3T3-E1 cells (0.1:1, 0.5:1, 1:1, 10:1, 100:1) for Transwell. In order to determine the optimal co-culture concentration of hUC-MSCs, the survival rate of MC3T3-E1 cells was determined by CCK8 and the apoptotic rate was detected using a flow cytometer. Dex was found to be able to reduce osteoblast survival and induce apoptosis of osteoblast, and HUC-MSCs prevented osteoblasts from survival reduction and apoptosis caused by Dex (Fig. 3A). The most effective concentration was found to be the hUC-MSCs and MC3T3-E1 cells that were co-cultured at 10:1, with a survival rate of  $66.047 \pm 0.028\%$  (Fig. 3C). With this concentration, the apoptotic rate was  $27.43 \pm 1.98\%$  (Fig. 3B).

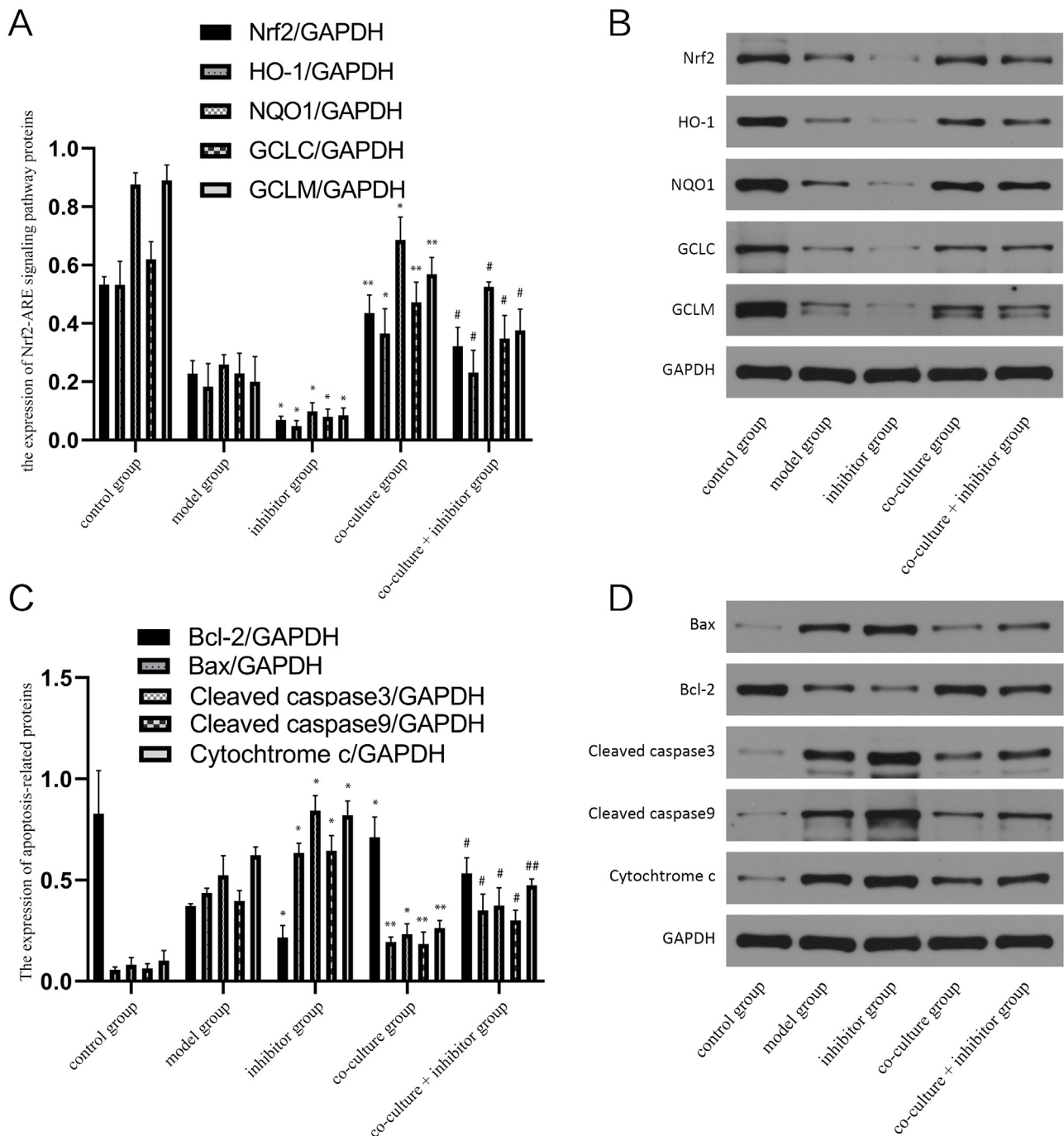


**Fig. 5.** Effects of hUC-MSCs on Nrf2-ARE signaling pathway proteins and apoptosis-related proteins. (A) Quantitative analysis of the expression levels of the Nrf2-ARE signaling pathway proteins of MC3T3-E1 cells,  $n = 3$ . (B) Expression levels of the Nrf2-ARE signaling pathway proteins were determined by Western blotting. (C) Quantitative analysis of the expression levels of apoptosis-related proteins of MC3T3-E1 cells,  $n = 3$ . (D) Expression levels of apoptosis-related proteins were determined by Western blotting.

### 3.4. HUC-MSCs inhibited Dex-induced apoptosis and oxidative stress in MC3T3-E1 cells and improved the activity of antioxidant enzymes

A flow cytometer was used for detecting apoptosis and ROS level in the MC3T3-E1 cells (Fig. 4A–D). Dex was found to significantly induce apoptosis and oxidative stress in MC3T3-E1 cells, while when ML385 was added, the apoptotic rate and ROS level of MC3T3-E1 cells were even higher. In comparison to the model group, the apoptotic rate and ROS level in the co-culture group were significantly reduced, which was then significantly increased following the addition of ML385 to

the co-culture system (Fig. 4A–D). These results suggest that hUC-MSCs inhibit apoptosis and oxidative stress in MC3T3-E1 cells induced by Dex.

As the CCK8 tests showed (Fig. 4E), Dex significantly reduced the survival of MC3T3-E1 cells, which were even lower following the addition of the Nrf2 inhibitor ML385. Compared to the model group, the survival rate in the co-culture group was significantly increased, suggesting that hUC-MSCs improve the survival of MC3T3-E1 cells induced by Dex. The survival rate was found to be significantly reduced after the addition of ML385 to the co-culture system.

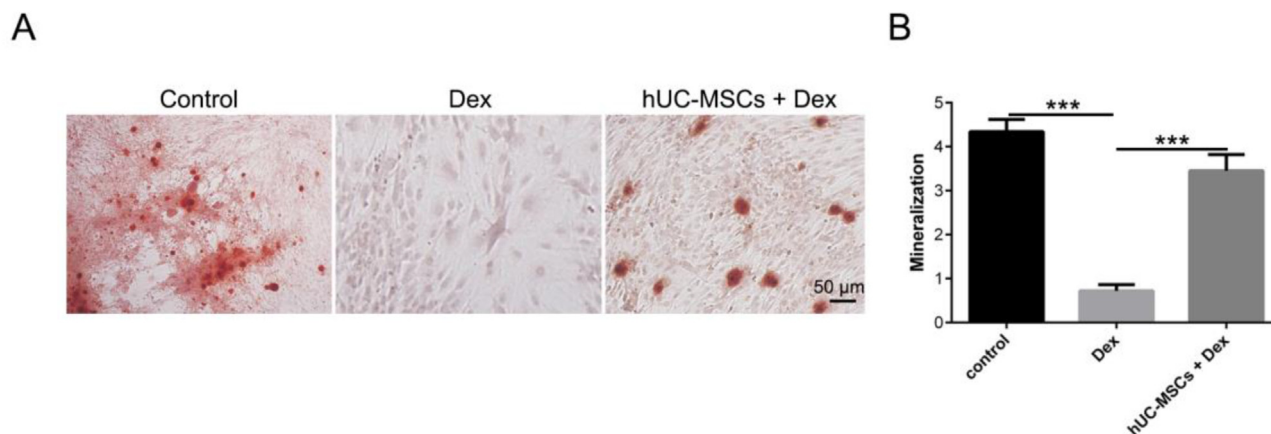


**Fig. 6.** Effect of hUC-MSCs on bone mineralization and osteogenesis ability. (A) Alizarin red staining for detecting calcified nodules in osteoblasts treated with Dex alone or in combination with hUC-MSCs, scale bar = 50 µm. (B) Quantitative analysis of osteoblast mineralization in (A),  $n = 3$ ,  $***P < 0.001$ .

The activity of antioxidase SOD, GSH-px, and CAT in each group was detected using biochemical assays (Fig. 4F). Dex significantly reduced the activity of antioxidase SOD, GSH-px, and CAT in MC3T3-E1 cells, which were even lower after the addition of ML385. In comparison to the model group, the activity of antioxidase SOD, GSH-px, and CAT in the co-culture group was significantly increased, which suggests that hUC-MSCs improve the activity of antioxidase SOD, GSH-px, and CAT in MC3T3-E1 cells. The activity of SOD, GSH-px, and CAT in MC3T3-E1 cells was found to be significantly reduced following the addition of ML385 to the co-culture system.

### 3.5. HUC-MSCs rescued the expression of apoptosis-related proteins and deactivation of the Nrf2-ARE signaling pathway induced by GCs

The apoptosis-related protein expression levels in each group were determined by Western blotting. Dex remarkably down-regulated the protein expression of bcl-2 and up-regulated the protein expressions of bax, cleaved caspase-3, cleaved caspase-9, and cytochrome C in MC3T3-E1 cells (Fig. 5C and D). However, after the addition of ML385, the bcl-2 protein expression was even lower and the expressions of bax, cleaved caspase-3, cleaved caspase-9, and cytochrome C was higher. In comparison to the model group, the bcl-2 protein expression in the co-culture group was found to be remarkably higher and the expressions of bax, cleaved caspase-3, cleaved caspase-9, and cytochrome C were remarkably lower. However, the bcl-2 protein expression was lower and the protein expressions of bax, cleaved caspase-3, cleaved caspase-9, and cytochrome C were higher following ML385 addition to the co-culture system (Fig. 5C and D).

In order to further explore the role of hUC-MSCs in the Nrf2-ARE signaling pathway and apoptosis caused by Dex, the expressions of Nrf2-ARE signaling pathway proteins in each group were also determined by Western blotting. Dex was found to have remarkably down-regulated the Nrf2 protein expression and those of its downstream proteins HO-1, NQO-1, GCLC, and GCLM in MC3T3-E1 cells (Fig. 5A and B). However, after the addition of ML385, the Nrf2, HO-1, NQO-1, GCLC, and GCLM protein expressions were all lower. Compared to the model group, the Nrf2, HO-1, NQO-1, GCLC, and GCLM protein expressions in the co-culture group were remarkably higher, while they were lower following the addition of ML385 to the co-culture system (Fig. 5A and B).

### 3.6. HUC-MSCs improves the ability of MC3T3-E1 cells to mineralize to osteogenesis under Dex treatment

The formation of 21 d mineralized deposits of MC3T3-E1 cells in the three groups was detected by alizarin red staining (Fig. 6A and B). The mineralized nodules were found to be larger, stained darker, and reddish-brown in the control group. Compared to the control group, Dex significantly inhibited the mineralization level of MC3T3-E1 cells, and no significant mineralized nodules were observed in the Dex group. In comparison to the Dex group, hUC-MSCs were found to significantly eliminate the mineralization of MC3T3-E1 cells inhibited by Dex, with significantly increased mineralization and deeper staining, which restored the osteoblast mineralization capacity in the hUC-MSCs + Dex group. These results demonstrate that hUC-MSCs can reverse the cytotoxicity of Dex while promoting mineralization in vitro.

### 3.7. HUC-MSCs reduce osteoblast apoptosis caused by dexamethasone via Nrf2-ARE activation

We used siRNA technology to knock down the Nrf 2 gene in hUC-MSCs to see whether the inhibitory effect of hUC-MSCs on dex-induced osteoblast apoptosis is related to the activation of Nrf 2. The results showed that after siRNA-NC transfection, hUC-MSCs could still promote the expression of Nrf 2, HO-1 and NQO 1 protein, reduce the apoptosis rate in MC3T3-E1 cells, and reduce the ROS level in MC3T3-E1 cells (Fig. 7A–C). However, after siRNA-Nrf 2 transfection, hUC-MSCs had no significant inhibition on the apoptosis and stress response induced by Dex in MC3T3-E1 cells, nor did the expression of Nrf 2, HO-1, and NQO 1 proteins (Fig. 7A–C). Therefore, we found that hUC-MSCs inhibited osteoblast apoptosis caused by Dex through activation of the Nrf 2-ARE pathway.

## 4. Discussion

The early treatment of GC-ONFH is of particular importance for relieving hip pain and claudication symptoms and preventing the further deterioration of femoral head necrosis, femoral head collapse, and the occurrence of osteoarthritis. Therefore, it is essential to prevent femoral head necrosis during the early stage of GC administration. In this study of rats, hUC-MSCs were

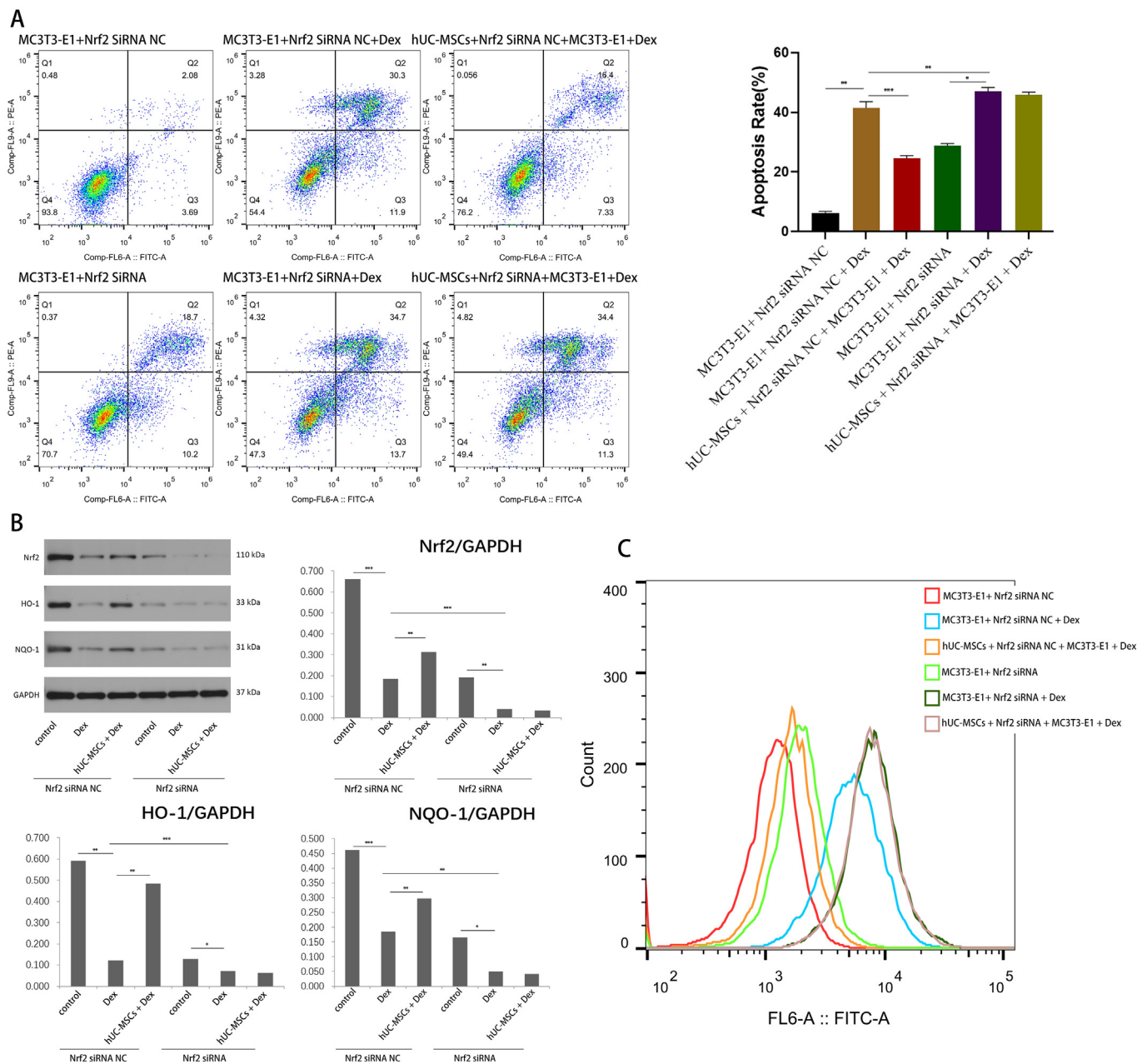


**Fig. 7.** HUC-MSCs inhibited osteoblast apoptosis caused by Dex through activation of the Nrf 2-ARE pathway. (A) MC3T3-E1 cell apoptosis in the 6 group was detected using flow cytometry. (B) Expression levels of the Nrf2-ARE signaling pathway proteins were determined by Western blotting. (C) ROS level of MC3T3-E1 cells measured by flow cytometry.

administered intravenously at the time of intramuscular GCs. HUC-MSCs were found to reduce the rates of empty bone lacuna and osteoblast apoptosis induced by GCs, while also improving femoral head bone density to effectively reduce the incidence of GC-ONFH. ALP is a marker of reactive osteoblast activity that is secreted by osteoblasts, and elevated ALP activity levels and mineralization are essential for bone formation [26]. This study also found that GCs can inhibit the osteogenic capacity of rat osteoblasts, thereby reducing ALP generation and activity. HUC-MSCs can effectively stimulate ALP activity in rats and calcium nodule formation in MC3T3-E1 cells. It was demonstrated that hUC-MSCs are effective against GC-ONFH at the animal level. The effectiveness of hUC-MSCs against GC-ONFH at the cell level and the mechanism were also further demonstrated.

The pathogenesis of GC-ONFH is complicated and not entirely clear. However, in the deep study of intracellular signaling pathways, initial progress has been made in the related pathways of GC-ONFH. Many reports have proven GC-ONFH to be involved in multiple pathways, and its ability to induce osteoblast apoptosis [6,24,28]. Oxidative stress is one of the important GC-ONFH mechanisms. When a cell is stimulated externally, a large amount of reactive oxygen species is produced in it, which can destroy the balance of oxidation and antioxidants in the cell and result in oxidative stress [7,8,11]. ROS has a tendency to damage the mitochondrial membrane and mitochondrial DNA, but it also increases the release of cytochrome C and alters the permeability of the mitochondria. The structure and function of the mitochondria are then disrupted, resulting in apoptosis [1].

There is a complex transcriptional regulatory network within cells that ensures oxidative stress remains at a normal level intracellularly [13]. One of the most important transcription factor regulatory pathways is the Nrf2 antioxidant response element (Nrf2-ARE). As Nrf2 is involved in numerous exogenous responses, it is considered to be a major cellular regulator against oxidative stress [25]. It was first identified as an obligatory protein that is required for a high level of globin gene expression in developing erythrocytes [16]. As studies progressed, Nrf2 was found to play a crucial role in carbohydrate metabolism and cell proliferation in DNA repair, mitochondrial function, and maintaining cellular redox homeostasis [5]. The Nrf2-ARE signaling pathway mainly consists of Nrf2, Kelch-like ECH-associated protein-1 (KEAP1), and ARE. KEAP1 acts as an inhibitory protein of Nrf2 and binds to it under normal physiological conditions, which causes Nrf2 to anchor to the cytosol, which is the predominant form of Nrf2 in the cytoplasm [10]. When cells are under oxidative stress, there is an increase in ROS levels and Nrf2 is phosphorylated into the nucleus. Nrf2 binds to ARE as a means of initiating the expression of a series of phase II detoxification enzymes and antioxidant genes, including HO-1, NQO-1, GCLC, and GCLM, to antagonize the oxidation effect of ROS and protect cells from oxidative damage [23]. In this study, Dex that increased ROS levels decreased the activity of the antioxidant enzymes SOD, GSH-Px, and CAT, while down-regulating the expression of the antioxidant protein Nrf2 and its downstream proteins HO-1, NQO-1, GCLC, and GCLM in MC3T3-E1 cells. Leading to oxidative stress. At the same time, Dex induced apoptosis of MC3T3-E1 cells by down-regulating bcl-2 protein expressions and up-regulating the protein expressions of bax, cleaved caspase-3, cleaved caspase-9, and cytochrome C. However, when ML385 was added, the indicators of oxidative stress and apoptosis further deteriorated. These results suggest that Nrf2-ARE signaling plays a major role in Dex-induced oxidative stress on osteoblasts, which leads to apoptotic apoptosis.

The role of MSCs in ameliorating oxidative stress damage has received a great deal of attention in recent times. Several studies have demonstrated that MSCs have a high antioxidant capacity because of their direct scavenging of free radicals [3]. The antioxidant effects of MSCs are potentially related to the paracrine function of MSCs. In a model of kidney injury due to ureteral obstruction, the administration of MSCs medium reduces lipid peroxidation [12]. Exosomes that are derived from the MSCs effectively reduce the oxidation of proteins and the peroxidation of lipids in animal models of sepsis, hyperglycemic brain injury, and cognitive impairment [2,18]. MSCs have also been found to reduce oxidative stress damage by scavenging free radicals, enhancing host antioxidant defense, regulating inflammatory responses, and enhancing mitochondrial function as a means of protecting damaged cells [4,9,14,19,21]. In this study, hUC-MSCs were found to reduce oxidative stress in MC3T3-E1 cells through the up-regulation of Nrf2 protein expression and those of its downstream proteins HO-1, NQO-1, GCLC, and GCLM in MC3T3-E1 cells. At the same time, hUC-MSCs inhibited the apoptosis of MC3T3-E1 cells by up-regulating bcl-2 protein expression and down-regulating the protein expressions of bax, cleaved caspase-3, cleaved caspase-9, and cytochrome C. These results suggest that hUC-MSCs reduce the level of oxidative stress that is caused by Dex and protect osteoblasts from apoptosis via the Nrf2-ARE signaling pathway.

## Funding

This study was funded by grants from the Henan Provincial Science and Technology Research Project (Scientific and Technological Research, 232102310327).

## CRedit authorship contribution statement

Chen Qiu: Conceptualization, Methodology, Formal analysis, Investigation, Writing – original draft preparation, Writing – review & editing. Xiaoming Yang: Methodology, Formal analysis, Investigation, Writing – review & editing. Puji Peng: Conceptualization, Methodology, Formal analysis, Investigation, Resources, Supervision, Writing – original draft preparation, Writing – review & editing. All authors have read and agreed to the final submitted version of the paper.

## Ethics approval

This study obtained ethics approval from the Institutional Animal Care and Use Committee (IACUC) of Wuhan University (Wuhan, China) (No. 20180920) and was in accordance with guidance that was issued by State Laboratory Animal Welfare Ethics.

## Data availability

Data will be made available on request.

## Declaration of competing interest

The authors declare that they have no known competing financial interests or personal relationships that could have appeared to influence the work reported in this paper. All authors guarantee the originality of the study and ensure that it has not been published previously. All the listed authors have read and approved the submitted manuscript.

## Acknowledgements

The authors wish to thank the Henan Provincial Science and Technology Research Project Foundation of Henan Provincial People's Hospital in China for their support.

## References

- [1] Brand MD, Affourtit C, Esteves TC, Green K, Lambert AJ, Miwa S, Pakay JL, Parker N. Mitochondrial superoxide: production, biological effects, and activation of uncoupling proteins. *Free Radic Biol Med* 2004;37:755–67.
- [2] Chang CL, Chen HH, Chen KH, Chiang JY, Li YC, Lin HS, Sung PH, Yip HK. Adipose-derived mesenchymal stem cell-derived exosomes markedly protected the brain against sepsis syndrome induced injury in rat. *Am J Transl Res* 2019;11:3955–71.
- [3] Chen MF, Lin CT, Chen WC, Yang CT, Chen CC, Liao SK, Liu JM, Lu CH, Lee KD. The sensitivity of human mesenchymal stem cells to ionizing radiation. *Int J Radiat Oncol Biol Phys* 2006;66:244–53.
- [4] DeSantiago J, Bare DJ, Banach K. Ischemia/Reperfusion injury protection by mesenchymal stem cell derived antioxidant capacity. *Stem Cells Dev* 2013;22:2497–507.
- [5] Dodson M, de la Vega MR, Cholanians AB, Schmidlin CJ, Chapman E, Zhang DD. Modulating NRF2 in disease: timing is everything. *Annu Rev Pharmacol Toxicol* 2019;59:555–75.
- [6] Guruvayoorappan C, Pradeep CR, Kuttan G. 13-cis-retinoic acid induces apoptosis by modulating caspase-3, bcl-2, and p53 gene expression and regulates the activation of transcription factors in B16F-10 melanoma cells. *J Environ Pathol Toxicol Oncol* 2008;27:197–207.
- [7] Ichiseki T, Kaneuji A, Katsuda S, Ueda Y, Sugimori T, Matsumoto T. DNA oxidation injury in bone early after steroid administration is involved in the pathogenesis of steroid-induced osteonecrosis. *Rheumatology (Oxford)* 2005;44:456–60.
- [8] Ichiseki T, Matsumoto T, Nishino M, Kaneuji A, Katsuda S. Oxidative stress and vascular permeability in steroid-induced osteonecrosis model. *J Orthop Sci* 2004;9:509–15.
- [9] Iyer SS, Torres-Gonzalez E, Neujahr DC, Kwon M, Brigham KL, Jones DP, Mora AL, Rojas M. Effect of bone marrow-derived mesenchymal stem cells on endotoxin-induced oxidation of plasma cysteine and glutathione in mice. *Stem Cells Int* 2010;2010:868076.

- [10] Keum YS, Choi BY. Molecular and chemical regulation of the Keap1-Nrf2 signaling pathway. *Molecules* 2014;19:10074–89.
- [11] Kim TH, Hong JM, Oh B, Cho YS, Lee JY, Kim HL, Shin ES, Lee JE, Park EK, Kim SY. Genetic association study of polymorphisms in the catalase gene with the risk of osteonecrosis of the femoral head in the Korean population. *Osteo Cartilage* 2008;16:1060–6.
- [12] Liu B, Ding FX, Liu Y, Xiong G, Lin T, He DW, Zhang YY, Zhang DY, Wei GH. Human umbilical cord-derived mesenchymal stem cells conditioned medium attenuate interstitial fibrosis and stimulate the repair of tubular epithelial cells in an irreversible model of unilateral ureteral obstruction. *Nephrology (Carlton)* 2018;23:728–36.
- [13] Ma Q. Role of nrf2 in oxidative stress and toxicity. *Annu Rev Pharmacol Toxicol* 2013;53:401–26.
- [14] Mahrouf-Yorgov M, Augeul L, Da SC, Jourdan M, Rigolet M, Manin S, Ferrera R, Ovize M, Henry A, Guuguin A, Meningaud JP, Dubois-Rande JL, Motterlini R, Foresti R, Rodriguez AM. Mesenchymal stem cells sense mitochondria released from damaged cells as danger signals to activate their rescue properties. *Cell Death Differ* 2017;24:1224–38.
- [15] Martire A, Bedada FB, Uchida S, Poling J, Kruger M, Warnecke H, Richter M, Kubin T, Herold S, Braun T. Mesenchymal stem cells attenuate inflammatory processes in the heart and lung via inhibition of TNF signaling. *Basic Res Cardiol* 2016;111:54.
- [16] Moi P, Chan K, Asunis I, Cao A, Kan YW. Isolation of NF-E2-related factor 2 (Nrf2), a NF-E2-like basic leucine zipper transcriptional activator that binds to the tandem NF-E2/AP1 repeat of the beta-globin locus control region. *Proc Natl Acad Sci U S A* 1994;91:9926–30.
- [17] Moya-Angeler J, Gianakos AL, Villa JC, Ni A, Lane JM. Current concepts on osteonecrosis of the femoral head. *World J Orthop* 2015;6:590–601.
- [18] Nakano M, Nagaishi K, Konari N, Saito Y, Chikenji T, Mizue Y, Fujimiya M. Bone marrow-derived mesenchymal stem cells improve diabetes-induced cognitive impairment by exosome transfer into damaged neurons and astrocytes. *Sci Rep* 2016;6:24805.
- [19] Pulavendran S, Vignesh J, Rose C. Differential anti-inflammatory and anti-fibrotic activity of transplanted mesenchymal vs. hematopoietic stem cells in carbon tetrachloride-induced liver injury in mice. *Int Immunopharmacol* 2010;10:513–9.
- [20] Shah KN, Racine J, Jones LC, Aaron RK. Pathophysiology and risk factors for osteonecrosis. *Curr Rev Musculoskelet Med* 2015;8:201–9.
- [21] Shalaby SM, El-Shal AS, Abd-Allah SH, Selim AO, Selim SA, Gouda ZA, Abd EMD, Zanfaly HE, El-Assar HM, Abdelazim S. Mesenchymal stromal cell injection protects against oxidative stress in *Escherichia coli*-induced acute lung injury in mice. *Cytotherapy* 2014;16:764–75.
- [22] Si X, Liu X, Li J, Wu X. Transforming growth factor-beta1 promotes homing of bone marrow mesenchymal stem cells in renal ischemia-reperfusion injury. *Int J Clin Exp Pathol* 2015;8:12368–78.
- [23] Tkachev VO, Menshchikova EB, Zenkov NK. Mechanism of the Nrf2/Keap1/ARE signaling system. *Biochemistry (Mosc)* 2011;76:407–22.
- [24] Tsuji M, Ikeda H, Ishizu A, Miyatake Y, Hayase H, Yoshiki T. Altered expression of apoptosis-related genes in osteocytes exposed to high-dose steroid hormones and hypoxic stress. *Pathobiology* 2006;73:304–9.
- [25] Vomund S, Schafer A, Parnham MJ, Brune B, von Knethen A. Nrf2, the master regulator of anti-oxidative responses. *Int J Mol Sci* 2017;18.
- [26] Wang T, Yang X, Qi X, Jiang C. Osteoinduction and proliferation of bone-marrow stromal cells in three-dimensional poly (epsilon-caprolactone)/hydroxyapatite/collagen scaffolds. *J Transl Med* 2015;13:152.
- [27] Wen Q, Zhou L, Zhou C, Zhou M, Luo W, Ma L. Change in hepatocyte growth factor concentration promote mesenchymal stem cell-mediated osteogenic regeneration. *J Cell Mol Med* 2012;16:1260–73.
- [28] Zalavras C, Shah S, Birnbaum MJ, Frenkel B. Role of apoptosis in glucocorticoid-induced osteoporosis and osteonecrosis. *Crit Rev Eukaryot Gene Expr* 2003;13:221–35.
- [29] Zhao H, He Z, Huang D, Gao J, Gong Y, Wu H, Xu A, Meng X, Li Z. Infusion of bone marrow mesenchymal stem cells attenuates experimental severe acute pancreatitis in rats. *Stem Cells Int* 2016;2016:7174319.